Low-resistance magnetic tunnel junctions with an MgO-Al$_2$O$_3$ composite tunnel barrier: Asymmetric transport characteristics and free electron modeling of a self-limited oxidation bilayer

C. de Buttet, M. Hehn, F. Montaigne, C. Tiusan, G. Malinowski, and A. Schuhl

Laboratoire de Physique des Matériaux, UMR CNRS 7556, B.P. 239, 54506 Vandœuvre lès Nancy Cedex, France

E. Snoeck

CEMES-CNRS-Groupe NanoMatériaux, 29 rue Jeanne Marvig, B.P. 94347, F-31055 Toulouse Cedex, France

S. Zoll

CROLLES 2, FREESCALE-PHILIPS-STMICROELECTRONICS, 850 rue Jean Monnet, F-38926 CROLLES Cedex, France

Low-resistance magnetic tunnel junctions with an MgO-Al$_2$O$_3$ composite tunnel barrier have been grown. From the theoretical point of view, current-voltage and magnetoresistance-voltage characteristics are predicted to be asymmetric. These asymmetries are studied as a function of barrier thicknesses for given experimental MgO and Al$_2$O$_3$ barrier heights. From an experimental point of view, the bottom alumina barrier acts as a diffusion barrier allowing the complete oxidation of the thin deposited Mg layer. As a result, composite Al$_2$O$_3$/MgO tunnel barriers show a lower area resistance and a magnetoresistance signal at nonzero applied voltage that is predicted to be equivalent as single Al$_2$O$_3$ tunnel barriers with the same total thickness. Current-voltage and magnetoresistance-voltage characteristics are shown to be asymmetric at high voltages.

PACS number(s): 85.75.$-$d, 72.25.$-$b

I. INTRODUCTION

The discovery of a tunnel magnetoresistance (TMR) effect at room temperature in oxide barrier based magnetic tunnel junctions[1] (MTJ) paved the way to intense developments in this field area with many possible application prospects.[2] Those numerous studies devoted to different aspects of this topic permit us to get a better understanding of the fundamentals of spin polarized tunneling transport. A large effort was paid to optimize the growth of thin insulating materials[1,3–5] and to model the magnetotransport properties across those tunnel barriers.[6,7] Much of the attention was then paid on the study of single tunnel barrier structures and the quality of the grown materials allows us now to pass a further step.

The next step consists to associate two or more tunnel barriers made with different materials in a single structure. Results have been reported on two terminal double tunnel barriers[8,9] or double Schottky barriers[10] and also on three terminal double tunnel barriers[11] or tunnel barrier/Schottky barrier.[12] Here, the tunnel barriers and/or Schottky barriers are separated by a metallic or magnetic layer or multilayer. Up to now, no real and complete experimental report on composite barriers, made of a multilayered insulator, has been done. One bottle neck relays on the difficulty to grow a dielectric layer on top of another one. Indeed, the dielectric layer is commonly made by post-deposition oxidation of a metallic layer. While the growth of a first dielectric layer of a dielectric bilayer is straightforward, the growth of the second one is hindered by the difference in surface energy between the first dielectric material and the metallic atoms of the second material before oxidation. This leads often to a growth of a discontinuous layer and nucleation of

clusters.[13,8] Previous studies have shown that in composite Al$_2$O$_3$/TaO barriers,[14] the magnetoresistance versus applied voltage asymmetries are linked to the insulator band structure. However, composite tunnel junctions are expected to show intrinsically highly nonsymmetric electrical characteristics[7] and it would have an important technological impact in spintronics applications.[8]

In this paper, we report on the theoretical and experimental magnetotransport properties of low-resistance magnetic tunnel junctions with an MgO-Al$_2$O$_3$ composite tunnel barrier.

From the theoretical point of view, current-voltage, $I(V)$, and magnetoresistance-voltage, TMR(V), characteristics are predicted to be asymmetric and this is directly linked to the difference in barrier heights of Al$_2$O$_3$ and MgO. The origin of asymmetries will be discussed. These asymmetries are modeled as a function of barrier thicknesses for given experimental microcrystalline MgO and amorphous Al$_2$O$_3$ barrier heights measured directly in previous studies.[4,5] The asymmetry of the TMR(V) and especially the location of the maximum of TMR at finite bias voltage could be used in applications if this potential corresponds to the working potential of the device.

From an experimental point of view, this study follows the one made on single microcrystalline MgO magnetic tunnel barriers.[5] Those junctions exhibit an area resistance of 10^5 Ω μm^2 for a 1.6 nm thick MgO barrier. Nevertheless we were not able to grow fully oxidized MgO layers with thicknesses less than 1.6 nm mainly because of the hard oxidation conditions of a pure dc plasma glow discharge. Indeed, the oxidation conditions lead to instantaneous over oxidized junctions perpendicular to the Co/Mg interface while lateral oxidation of the Mg layer is not completed. This is explained
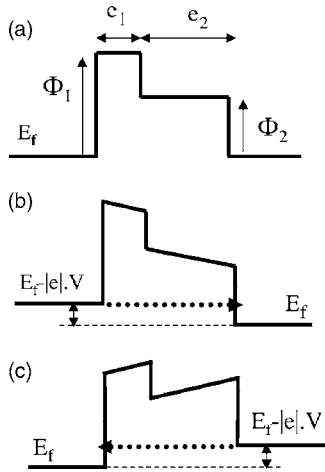
FIG. 1. Composite tunnel barrier potential profile at zero applied voltage (a), under a positive applied voltage (b), and under a negative applied voltage (c).

FIG. 2. Computed current density as a function of applied voltage in a composite $Al_2O_3(x \text{ nm})/MgO(1.6 \ x \text{ nm})$ tunnel junctions for $x=1.2$ nm, 0.8 nm, and $x=0.4$ nm. Inset (a), variation of the area resistance as a function of x; inset (b), variation of the maximum current asymmetry as a function of x.

by the preferential oxidation at Mg grain bounderies. Then, adding a bottom alumina barrier will act as a diffusion barrier allowing the complete oxidation of the thin deposited Mg layer. As a result, composite Al_2O_3/MgO tunnel barriers show lower area resistance and predicted equivalent magnetoresistance signal at nonzero applied voltage as single Al_2O_3 tunnel barriers with the same thickness.

II. THE COMPOSITE BARRIER—TOWARDS ASYMMETRIC MAGNETOTRANSPORT CHARACTERISTICS

Composite barriers are made of a bilayer or of a multilayer composed with two or more insulating materials. In the case addressed in the present work, a bilayer is made of two insulators with different barrier heights. This configuration leads to the asymmetrical potential profile given in Fig. 1(a). The effective barrier heights are fixed and measured to be equal to $\phi_{Al_2O_3}=1.5$ eV and $\phi_{MgO}=0.7$ eV from our previous experimental measures.[4,5] Then, the respective thicknesses of both barriers can be varied and effects on the magnetotransport characteristics of the composite tunnel junction can be theoretically evaluated. It has been shown that either through Al_2O_3 or MgO, the electron tunneling can be modeled with the parabolic band model using such effective tunnel barrier heights.[7,5] Indeed, spin filtering by the tunnel barrier associated to the symmetry of the system and the associated high magnetoresistance ratio require epitaxial magnetic tunnel junctions[15] or highly textured.[16] As soon as a polycrystalline and/or an amorphous barrier is grown, band effects are smeared out and the parabolic band model applies with effective barrier height and thickness. These parameters are the result of an average over the tunnel junction surface of the wave vector dependent tunnel probabilities. Finally, the parabolic band model is suitable to take into account such complex barrier potentials but also the distortion of the barrier under an applied voltage. The model is described in detail in Refs. 7 and 17. Briefly speaking, it relies on elastic coherent tunneling in a laterally invariant system. The total
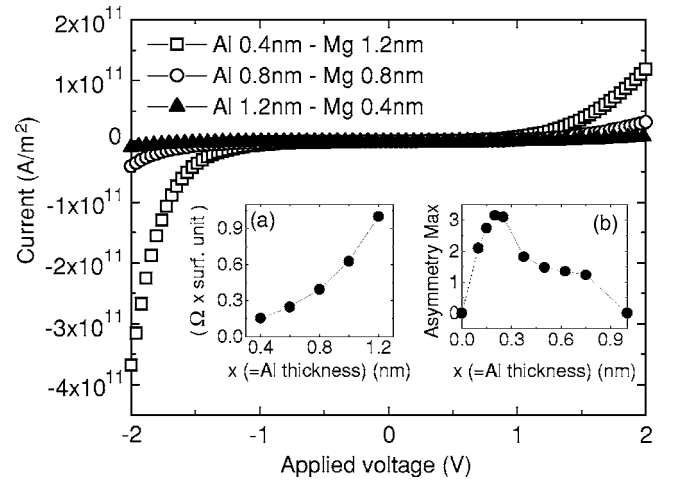
energy and the transverse wave vector are thus conserved in the process. The transmission coefficient is computed by resolving analytically the Schrödinger equation considering linear potential and exchange splitting for the magnetic electrodes. The transmission coefficient is integrated over the possible energies for a zero temperature. For the band structure of the electrodes, parameters proposed by Davies and MacLaren[18] are used; for the barriers, a normalized effective mass of 0.4 is assumed.

In a first step, the modeling of a 1.6 nm thick composite barrier $Al_2O_3(x \text{ nm})/MgO(1.6 \ x \text{ nm})$ is presented. This highlights the tendencies of the resistance, the current asymmetry, and the TMR ratio and shift when x is varied. First of all, the $I(V)$ characteristics exhibit an asymmetric behavior as shown in Fig. 2. This asymmetry is directly linked to the asymmetric barrier potential. When the barrier is negatively biased as in Fig. 1(b), the effective barrier height and thickness decrease with the potential increase. This leads to a strong increase in the tunnel current. When the barrier is positively biased as in Fig. 1(c), the effective barrier height and thickness are quite constant as the potential increases before a reduction at high potential. As a consequence, the $I(V)$ characteristic appears to be asymmetric. The composite barrier area resistance increases strongly with the Al_2O_3/MgO thickness ratio [inset (a), Fig. 2]. The more the aluminum layer is thick, the more the resistance is high. Obviously, increasing x increases the mean barrier height and so the barrier resistance. Then, if a low resistance tunnel barrier is desired, a weak proportion of Al_2O_3 would be preferred. The $I(V)$ asymmetric behavior is quantified by the current asymmetry ratio $\alpha(V)=I(V)/-I(-V)$.

This asymmetry first increases as the thickness of MgO increases, reaches a maximum and then decreases. In inset (b) of Fig. 2, we report the maximum of asymmetry as a function of x. This behavior has been observed even for a broad range of the whole barrier. As shown in Fig. 3, the $TMR(V)$ characteristics are asymmetric and, interestingly,
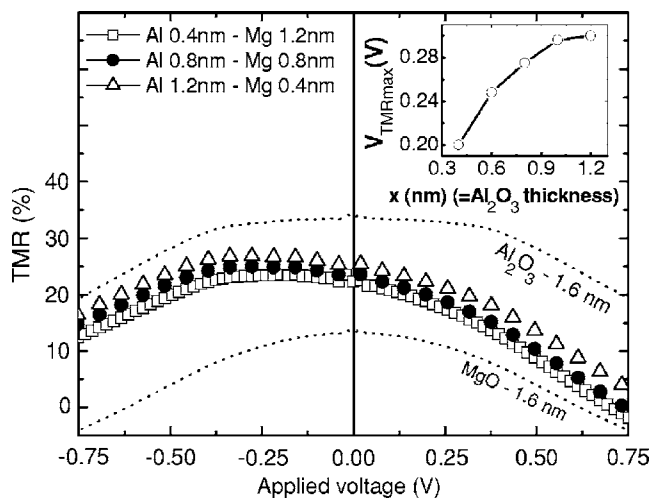
FIG. 3. Computed variation of the tunnel magnetoresistance, TMR, as a function of applied voltage in a composite $Al_2O_3(x$ nm$)/MgO(1.6\ x$ nm$)$ tunnel junctions for $x=1.2$ nm, 0.8 nm, and $x=0.4$ nm. Inset: variation of $V_{TMR\ max}$ as a function of x. The TMR(V) for single 1.6 nm thick Al_2O_3 and MgO barriers have been added in as dotted lines in the figure.

the maximum value of TMR is not reached at zero bias voltage but for a value, labeled $V_{TMR\ max}$, which depends on x. The inset of Fig. 3 shows the variation of $V_{TMR\ max}$ with x. Both the maximum of TMR and $V_{TMR\ max}$ increase with x, the thickness of the Al_2O_3 part of the 1.6 nm thick composite barrier. The drift of $V_{TMR\ max}$ towards high potential is beneficial if we consider that the maximum of TMR could be available if the device works under a bias voltage more or less equal to the $V_{TMR\ max}$. In brief, this result encourages the elaboration of hybrid junctions with large Al_2O_3 proportion.

In a second step, the modeling of a composite barrier with constant Al_2O_3/MgO thickness ratio but varying total thickness has been done. From the previous paragraph, it can be seen that if the purpose consists to grow low resistive junctions with visible current asymmetries, the composite barrier must be made with a MgO layer thicker than the Al_2O_3 one. Therefore, an Al_2O_3/MgO thickness ration of 0.33 has been chosen in the following calculations. Resistance versus total composite barrier thickness is not reported here since the result is straightforward. Indeed, obviously, the junction resistance increases exponentially with its barrier thickness. In Fig. 4(a), it appears clearly that the current asymmetry increases when the total thickness increases. It is worth noting that the maximum of $\alpha(V)$ shifts to low applied voltage when thickness increases. As far as TMR is concerned, its value globally increases when the thickness of the whole stack decreases. This result was already shown in single MTJ.[7] The inset of Fig. 4(b) shows the variation of $V_{TMR\ max}$ with the total composite barrier thickness. In this case, $V_{TMR\ max}$ decreases as the total thickness increases. The drift of $V_{TMR\ max}$ towards high potential is beneficial if we consider that the maximum of TMR could be used if the device works under a bias voltage more or less equal to the $V_{TMR\ max}$. This result encourages the elaboration of hybrid junction with low total composite barrier thickness.

In summary, the theoretical calculations on magnetotransport characteristics of composite Al_2O_3/MgO tunnel barriers
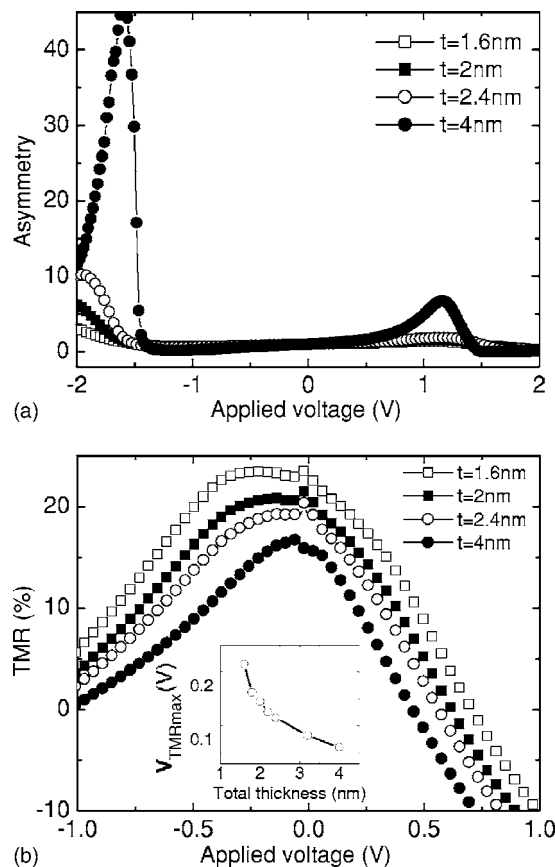

FIG. 4. (a) Calculated variation of current asymmetry with applied voltage for $Al_2O_3[(3t/4)$ nm$]/MgO[(t/4)$ nm$]$ tunnel junctions for $t=1.6$ nm, 2 nm, 2.4 nm, and 4 nm. (b) Calculated variation of magnetoresistance with applied voltage for $Al_2O_3[(3t/4)$ nm$]/MgO[(t/4)$ nm$]$ tunnel junctions for $t=1.6$ nm, 2 nm, 2.4 nm, and $t=4$ nm. Inset: variation of $V_{TMR\ max}$ as a function of t.

predict that: (i) with fixed Al_2O_3/MgO thickness ratio, high $\alpha(V)$ is supported by a thick barrier while high TMR and $V_{TMR\ max}$ are supported by a thin barrier; (ii) with fixed total barrier thickness, both TMR and $V_{TMR\ max}$ increase with the Al_2O_3 layer thickness. From this conclusion, it is clear that combining a high TMR ratio with low area resistance, high $V_{TMR\ max}$ and high $\alpha(V)$ within a given composite barrier is hard to achieve. So priorities have been defined for experimental investigations. First, in the continuity of our work on single MgO magnetic tunnel barriers,[5] a low area resistance suitable for future generations of magnetic random access memory (MRAM) is wanted. So the thinnest barriers have been grown. Then, in order to show the asymmetric character of the hybrid junctions, we promoted composite barriers with a MgO layer thickness larger than the Al_2O_3 layer thickness. This is also in agreement with an Al_2O_3 layer used as a diffusion barrier rather than to increase the TMR signal of the composite barrier.

III. FORMATION OF A COMPOSITE ALUMINE/MAGNESIUM OXIDE BARRIER

Junctions are deposited onto float-glass substrates by sputtering tantalum, platinum, magnesium targets mounted

on rf magnetron cathodes and cobalt on a dc magnetron cathode. The base pressure is less than 5×10^{-7} mbar and the substrates are maintained at room temperature. The studied samples are composed of Glass/Ta(5 nm)/Pt(20 nm)/ Co(10 nm)/[Al(x nm)/Mg(y nm), oxidized t_{Ox} s]/ Co*(20 nm)/Pt(5 nm). All the layers are deposited at an operating pressure fixed to 5×10^{-3} mbar except the last Co layer of the stack, denoted by Co*, deposited at 1.5 $\times 10^{-2}$ mbar. When Co is deposited at low Ar pressure (5 $\times 10^{-3}$ mbar), the magnetization reversal is sharp with nucleation and propagation of domain walls. When the Ar pressure increases up to an optimum equal to 1.5×10^{-2} mbar, the grain size and the coercive field increase up to a maximum. In this way, two electrodes with different coercive fields can be made at each side of the barrier.[4]

To obtain the Al$_2$O$_3$/MgO composite barrier, the oxidation is made just after deposition of the metallic Al/Mg bilayer using a dc glow discharge at a power of 200 W and voltage of 600 V under a pure 10^{-1} mbar O$_2$ plasma in the sputtering load lock. The samples are transferred to this chamber without breaking the vacuum.

To define the junction geometry for electronic transport measurements, we have used *ex situ* changed contact masks with a path width of 200 μm. Each sample was prepared to include 14 tunnel junctions. Details on the junction geometry can be found elsewhere.[4] The electrical resistivity was measured with a standard four-probe dc technique.

Three series of composite barriers have been grown with deposited metal layers of Al(0.7 nm)/Mg(1.6 nm), Al(0.7 nm)/Mg(1.1 nm), and Al(0.5 nm)/Mg(1.4 nm). The properties of tunnel junctions formed from a single Al(0.7 nm) or Mg(1.6 nm) film have already been reported.[4,5] For each structure, the oxidation time t_{Ox} has been varied to achieve an optimal oxidation of the bilayer. The average values and standard deviation of resistance and magnetoresistance for different samples and different oxidation conditions are represented in Fig. 5. These values are based on measurements of 12 to 14 junctions per sample. For Al(0.7 nm)/Mg(1.6 nm) bilayer [Fig. 5(a)] an optimum TMR of 7% at room temperature could be measured with $t_{Ox}=48$ s. For longer oxidation times the MR is slightly reduced (6%) and the resistance seems to saturate from t_{Ox} >53 s. This saturation of the resistance and the weak decrease in magnetoresistance suggests that the Al layer acts as a diffusion barrier and prevents further oxidation of the bottom Co electrode. A similar behavior is observed for Al(0.7 nm)/Mg(1.1 nm) bilayers [Fig. 5(b)]. Due to the reduced Mg thickness, the resistance saturates around 20 kΩ (instead of 110 kΩ for a 1.6 nm thick Mg layer).

For a 0.5 nm thickness of aluminum, a different phenomenology is observed [Fig. 5(c)]. The resistances and the magnetoresistances are very dispersed for a same sample and the statistical properties vary from sample to sample (see, for example, 20 and 25 s). Unlike the previous case, a reduction of magnetoresistance is observed for longer oxidation times and larger resistances. Then, for a reduced Al thickness, this layer does not play its role of diffusion barrier and small process variations lead to different results concerning TMR ratio and junction area resistance. For such a thickness, con-
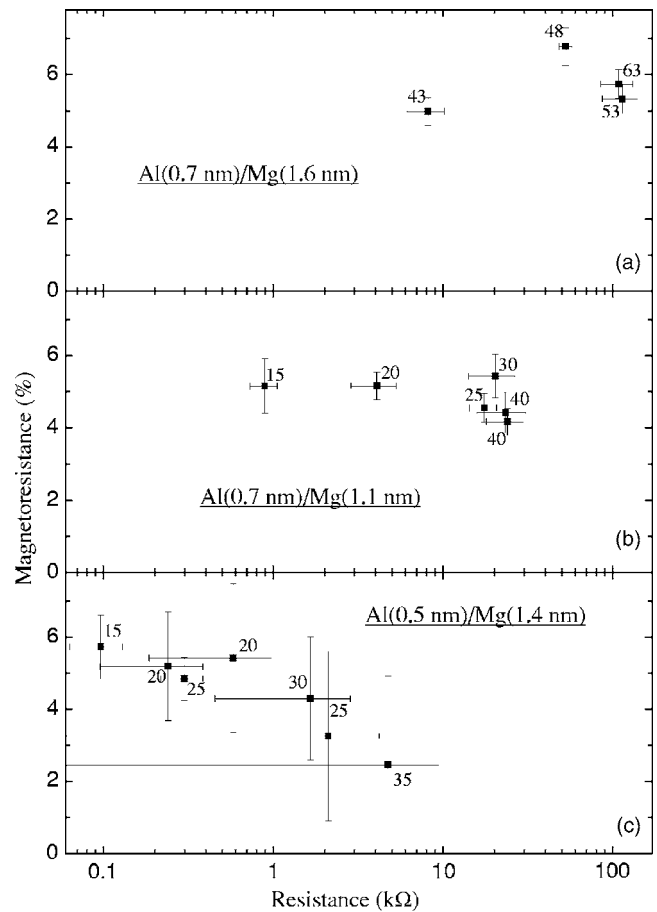

FIG. 5. Variation of the TMR as a function of junction resistance for tunnel composite barriers made with an oxidation of a Al(0.7 nm)/Mg(1.6 nm) bilayer (a), a Al(0.7 nm)/Mg(1.1 nm) bilayer (b), and a Al(0.5 nm)/Mg(1.4 nm) bilayer. In each curve, the numbers indicate the oxidation time.

sidering the roughness of the bottom electrode, the Al layer might not be continuous.

The structure and the microstructure of the stacking sequence were studied by transmission electron microscopy (TEM) on cross sectional samples prepared by the usual method, i.e., first mechanically thinned then ion milled down to the electron transparency. The TEM studies were performed using a FEI 200 kV field emission gun microscope fitted with a Cs corrector whose point resolution is 0.12 nm. The low magnification TEM image inset Fig. 6 illustrates the whole stacking sequence with quite rough interfaces while the high resolution TEM (HRTEM) micrograph shows the fine structure of the Al$_2$O$_3$+MgO barrier. As expected the alumina barrier is amorphous while crystalline MgO grains are visible. The crystalline fcc structure of Co is verified and no evidence of a possible oxidation of the bottom Co layer was observed proving the efficiency of Al$_2$O$_3$ as a diffusion barrier. Figure 6 shows clearly that the Al$_2$O$_3$/MgO interface is not well defined. This mixing can originate directly from the diffusion between Al and Mg during the growth before oxidation. Furthermore, the oxidation step can cause some mixing at the interfaces through the diffusion of Al or Mg atoms.
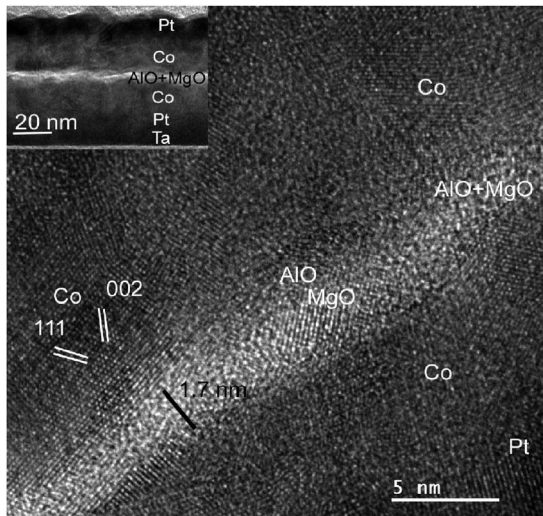
FIG. 6. HREM micrograph of the insulating composite barrier observed on a cross sectional MJT sample with a low TEM micrograph of the whole stacking in the inset.

This study has shown that it is possible to oxidize a metallic bilayer in a single oxidation step. Furthermore, a 0.7 nm thick Al layer acts as a diffusion barrier for oxygen preventing the oxidation of the bottom electrode. This effect is not observed for a single Al layer and is not related to the total thickness of the bilayer. This feature is thus specific to the nature of the bilayer.

We now detail magnetotransport properties for the optimized junctions.

IV. MAGNETOTRANSPORT IN A COMPOSITE BARRIER

The presence of TMR is an indication of the quality of the composite barrier formed by oxidation of the metallic bilayer. The surfacic resistance of a barrier formed from a Mg(1.6 nm) layer is 200 kΩ μm^2.[5] The high surface resistance of the composite barrier ($>$1 GΩ μm^2) thus proves that the composite barrier acts as a single tunnel barrier and that direct tunneling is the main mode of transport through the barrier. This increase of resistance by association of different barriers is quantitatively described by the parabolic band model (a difference of resistance by a factor of 10^4 exists between the composite Al$_2$O$_3$/MgO and the MgO single barrier and by a factor of 10^6 between the composite Al$_2$O$_3$/MgO and the Al$_2$O$_3$ single barrier). The prominence of direct tunneling in the transport is also confirmed by the temperature dependence of the resistance[19] (not shown). The resistance increases by a factor of 1.5 between 300 K and 77 K. According to Stratton,[20] this tunnel resistance increase at low temperature depends on the mean barrier height. With a composite tunnel barrier, the mean barrier height is located between MgO and Al$_2$O$_3$ barrier heights. Then, the resistance variation should also be between the one observed for single MgO and Al$_2$O$_3$ barriers. This is indeed the case with a resistance increase by a factor of 2 (respectively, 1.2) for a MgO (respectively, Al$_2$O$_3$) single barrier of the same total thickness.
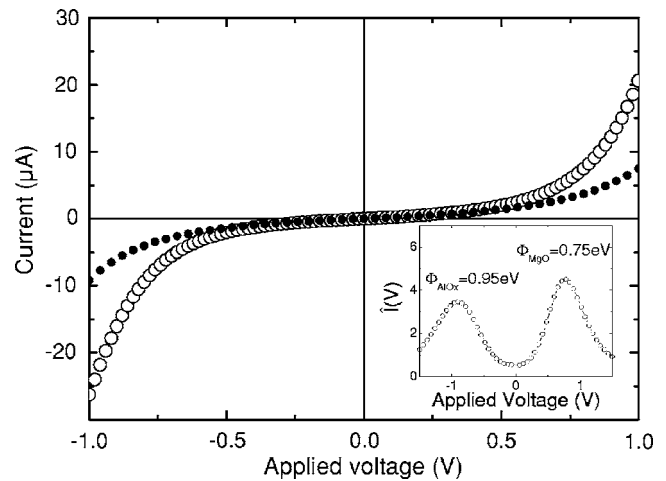

FIG. 7. Current as a function of applied voltage in a composite Al(0.7 nm)/Mg(1.6 nm) tunnel barrier with t_{Ox} equal to 48 s measured at 300 K (-○-) and 77 K (-●-). Inset: calculus of the $\hat{I}(V)$ also on the same junction.

Figure 7 shows the $I(V)$ characteristics measured at 77 and 300 K between -1 and $+1$ V for a Al(0.7 nm)/Mg(1.6 nm) bilayer. As expected, the characteristics are asymmetric. The maximum measured asymmetry is 1.9. This value is not a maximum as represented in Fig. 4 but is limited experimentally by the breakdown of the junctions (occurring at voltages around 1 V whereas from calculations maxima of asymmetry are expected at voltages beyond 1.5 V). For single barriers, effective barriers parameters are usually deduced from fits to analytical formula. Brinkman model[21] can be used to fit an asymmetric $I(V)$ characteristic with a third order polynomial. This leads in our case to a barrier height of 0.68 eV with barrier asymmetry of 1.28 eV and a barrier thickness of 2.8 nm. This expresses the asymmetry of the barrier but no information can be extracted from this fit. An original method, based on the temperature variation of the $I(V)$ characteristic, was used to determine the barrier height at each interface of the barrier. It can be shown that the temperature variation of the current, represented by $\hat{I}(V)=[I(V,T)-I(V,0)]/I(V,0)$, exhibit a maxima at a voltage related to the barrier height.[22] According to the sign of the applied bias voltage, the MgO interface or the Al$_2$O$_3$ interface can be probed. From the inset of Fig. 7, an Al$_2$O$_3$ barrier height of 1 eV is found which is a low value compared to former studies but the extracted MgO barrier height of 0.75 eV is in agreement with the previous study. This experiment confirms the different value of the barrier height at each interface and confirms once again that a composite barrier has been made.

The magnetoresistance ratio has been studied as a function of applied voltage for barriers formed by oxidation of Al(0.7 nm)/Mg(1.6 nm) and Al(0.7 nm)/Mg(1.1 nm) bilayers (Fig. 8). The TMR(V) is asymmetric, the magnetoresistance ratio is reduced to half of its maximum value at bias voltages $V_{1/2}$ of about 0.31 V at the Al$_2$O$_3$ and of about 0.21 V at the MgO interface. Those values are in agreement with those measured on single tunnel barriers (the parabolic band model predicts that the decrease rate of the magnetore-
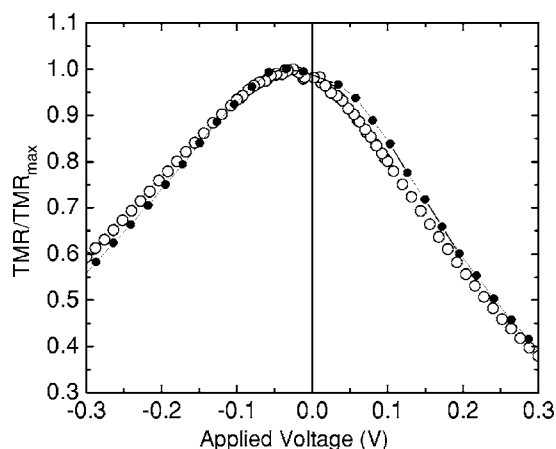
FIG. 8. Measure of the normalized TMR as a function of applied voltage at 300 K in a composite Al(0.7 nm)/Mg(1.6 nm) tunnel barrier with t_{Ox} equal to 48 s (-○-) and in a composite Al(0.7 nm)/Mg(1.1 nm) tunnel barrier with t_{Ox} equal to 20 s (-●-).

sistance for a given polarity depends essentially on the interface at which electrons are collected[17]). As expected, the maximum of magnetoresistance is slightly shifted from zero bias with a shift of 25 mV for Al(0.7 nm)/Mg(1.6 nm) bilayer and 45 mV for Al(0.7 nm)/Mg(1.1 nm) bilayer.

Asymmetries in the $I(V)$ characteristics are often observed in magnetic tunnel junctions. They have been associated to an imperfect oxidation of the barrier (nonuniform, over or under oxidized) or to nonsymmetric electrodes. To our knowledge, it is the first time that a shift of the maximum of magnetoresistance is observed for identical electrodes. Thanks to our systematic study of the oxidation, we can exclude that this asymmetry is related to an over or under oxidation of the Al or Mg layer.

The parabolic band model explains the increase of the TMR shift with the reduction of the MgO thickness. However, the values of the shift are lower than the ones predicted theoretically. This difference might be explained by the reduced value of the alumina barrier height (1 eV instead of 1.5 eV). The reduction of the difference in barrier between Al$_2$O$_3$ and MgO reduces obviously the asymmetry of the $I(V)$ and the shift of the maximum TMR. Using the barrier heights measured with the $\hat{I}(V)$ curves, the calculated $V_{TMR\ max}$ falls down to 50 mV instead of 140 mV. But this value is still higher than the 25 mV measured value. From

the TEM observations, it appears that the interface between Al$_2$O$_3$ and MgO is not perfectly abrupt and might be quite different from the perfect interface considered in the calculations. However, the effect of a nonabrupt interface on the parabolic band model is not that important. If it influences notably the asymmetry of $I(V)$ characteristic, especially for high biases, it has almost no influence on the shift of the maximum of TMR.

Another origin of the discrepancy between theory and experiments relies on the other possible mode of transport through the barrier as incoherent tunneling via one or several defects as localized state or inelastic tunnel assisted by phonons or magnons. The latter is mainly responsible for the decrease of magnetoresistance observed at low biases[23] in magnetic tunnel junctions. As the voltage dependence of this magnon assisted tunneling in this voltage range (below 100 mV) is essentially dominated by the structure of the magnon spectra and thus by the electrodes, this contribution to the current which reduces the magnetoresistance is symmetric. Magnon assisted tunneling can thus be responsible for the reduction of the TMR(V) shift.

V. CONCLUSIONS

In conclusion, we have successfully modeled and synthesized by sputtering composite Al$_2$O$_3$/MgO magnetic tunnel junctions. This has been done by using a common oxidation step for both Al and Mg layer. Regarding the Al layer, we have demonstrated that it can act as a good oxygen diffusion barrier, which enabled us to reduce the lower limit value of the thickness of a fully oxidized MgO layer. From our experimental point of view, we have made composite junctions with levels of resistance as low as comparable MgO magnetic tunnel junctions ($<10^7$ Ω μm^2 for 1.9 nm thick composite magnetic tunnel junction), and with levels of TMR equivalent to our Al$_2$O$_3$ based junctions (around 8%). Moreover, we have collected proofs of an hybrid junction tunneling and demonstrated experimentally that changes in the barrier thicknesses induces changes in terms of asymmetry behavior.

[1] J. S. Moodera, L. R. Kinder, T. M. Wong, and R. Meservey, Phys. Rev. Lett. **74**, 3273 (1995).

[2] S. A. Wolf, J. Supercond. **13**, 195 (2000).

[3] J. Nowak and J. Rauluszkiewicz, J. Magn. Magn. Mater. **109**, 79 (1992); J. S. Moodera and L. R. Kinder, J. Appl. Phys. **79**, 4724 (1996); C. L. Platt, B. Dieny, and A. E. Berkowitz, *ibid.* **81**, 5523 (1997); J. M. De Teresa, A. Barthélémy, A. Fert, J. P. Contour, R. Lyonnet, F. Montaigne, P. Seneor, and A. Vaurès, Phys. Rev. Lett. **82**, 4288 (1999); P. Rottländer, M. Hehn, O.

Lenoble, and A. Schuhl, Appl. Phys. Lett. **78**, 3274 (2001).

[4] M. Hehn, O. Lenoble, D. Lacour, C. Féry, M. Piécuch, C. Tiusan, and K. Ounadjela, Phys. Rev. B **61**, 11643 (2000).

[5] M. Hehn, C. de Buttet, G. Malinowski, E. Snoeck, C. Tiusan, and F. Montaigne, Eur. Phys. J. B **40**, 19 (2004).

[6] M. Jullière, Phys. Lett. **54A**, 225 (1975); J. C. Slonczewski, Phys. Rev. B **39**, 6995 (1989); I. I. Mazin, Phys. Rev. Lett. **83**, 1427 (1999); I. I. Oleinik, E. Y. Tsymbal, and D. G. Pettifor, Phys. Rev. B **62**, 3952 (2000); J. M. MacLaren, X. G. Zhang,

W. H. Butler, and X. Wang, *ibid.* **59**, 5470 (1999).

[7] F. Montaigne, M. Hehn, and A. Schuhl, Phys. Rev. B **64**, 144402 (2001).

[8] C. Tiusan, M. Chshiev, A. Iovan, V. da Costa, D. Stoeffler, T. Dimopoulos, and K. Ounadjela, Appl. Phys. Lett. **79**, 4231 (2001).

[9] F. Montaigne, J. Nassar, A. Vaurès, F. Nguyen Van Dau, F. Petroff, A. Schuhl, and A. Fert, Appl. Phys. Lett. **73**, 2829 (1998).

[10] D. J. Monsma, R. Vlutters, and J. C. Lodder, Science **281**, 407 (1998).

[11] M. Hehn, F. Montaigne, and A. Schuhl, Phys. Rev. B **66**, 144411 (2002); D. Lacour, M. Hehn, F. Montaigne, H. Jaffrès, P. Rottlander, G. Rodary, F. Nguyen Van Dau, F. Petroff, and A. Schuhl, Europhys. Lett. **60**, 896 (2002); S. Stein, R. Schmitz, and H. Kohlstedt, Solid State Commun. **117**, 599 (2001).

[12] S. van Dijken, X. Jiang, and S. S. P. Parkin, Phys. Rev. B **66**, 094417 (2002).

[13] P. LeClair, H. J. M. Swagten, J. T. Kohlhepp, R. J. M. van de Veerdonk, and W. J. M. de Jonge, Phys. Rev. Lett. **84**, 2933 (2000); and references therein.

[14] M. Sharma, S. X. Wang, and J. H. Nickel, Phys. Rev. Lett. **82**, 616 (1999).

[15] C. Tiusan, J. Faure-Vincent, C. Bellouard, M. Hehn, E. Jouguelet, and A. Schuhl, Phys. Rev. Lett. **93**, 106602 (2004); C. Tiusan, J. Faure-Vincent, M. Sicot, M. Hehn, C. Bellouard, F. Montaigne, S. Andrieu, and A. Schuhl, Mater. Sci. Eng., B **126**, 112 (2006).

[16] S. Yuasa, T. Nagahama, A. Fukushima, Y. Suzuki, and K. Ando, Nat. Mater. **3**, 868 (2004); S. S. P. Parkin, C. Kaiser, A. Panchula, P. M. Rice, B. Hughes, M. Samant, and S.-H. Yang, Nat. Mater. **3**, 862 (2004).

[17] F. Montaigne, M. Hehn, and A. Schuhl, J. Appl. Phys. **91**, 7020 (2002).

[18] A. H. Davies and J. M. MacLaren, J. Appl. Phys. **87**, 5224 (2000).

[19] J. J. Akerman, R. Escudero, C. Leighton, S. Kim, D. A. Rabson, R. W. Dave, J. M. Slaughter, and I. K. Schuller, J. Magn. Magn. Mater. **204**, 86 (2002).

[20] R. Stratton, Phys. Chem. Solids **23**, 1177 (1962).

[21] W. F. Brinkman, R. C. Dynes, and J. M. Rowell, J. Appl. Phys. **41**, 1915 (1971).

[22] P. Rottländer, M. Hehn, and A. Schuhl, Phys. Rev. B **65**, 054422 (2002).

[23] S. Zhang, P. M. Levy, A. C. Marley, and S. S. P. Parkin, Phys. Rev. Lett. **79**, 3744 (1997).